



MacLaren, I. , Nord, M., Jiao, C. and Yücelen, E. (2019) Liftout of high-quality thin sections of a perovskite oxide thin film using a xenon plasma focused ion beam microscope. *Microscopy and Microanalysis*, 25(1), pp. 115-118. (doi:[10.1017/S1431927618016239](https://doi.org/10.1017/S1431927618016239))

This is the author's final accepted version.

There may be differences between this version and the published version. You are advised to consult the publisher's version if you wish to cite from it.

<http://eprints.gla.ac.uk/179952/>

Deposited on: 01 April 2019

Enlighten – Research publications by members of the University of Glasgow  
<http://eprints.gla.ac.uk>

# Liftout of high quality thin sections of a perovskite oxide thin film using a Xenon Plasma Focused Ion beam microscope

Ian MacLaren<sup>1</sup>, Magnus Nord<sup>1</sup>, Chengge Jiao<sup>2</sup>, Emrah Yücelen<sup>2†</sup>

1. School of Physics and Astronomy, University of Glasgow, Glasgow G12 8QQ, UK

2. Materials & Structural Analysis, Thermo Fisher Scientific, Achtseweg Noord 5, 5651GG Eindhoven, Netherlands

## Abstract

It is shown that the Xenon plasma focused ion beam microscope is an excellent tool for high quality preparation of functional oxide thin films for atomic resolution electron microscopy. Samples may be prepared rapidly, at least as fast as those prepared using conventional gallium FIB. Moreover, the surface quality after 2 kV final polishing with the Xe beam is exceptional with only about 3 nm of amorphised surface present. The sample quality was of a suitably high quality to allow atomic resolution HAADF and iDPC without any further preparation, and the resulting images were good enough for quantitative evaluation of atomic positions to reveal the oxygen octahedral tilt pattern. This suggests that such Xenon plasma FIB instruments may find widespread application in TEM and STEM specimen preparation.

## Introduction

Focused ion beam (FIB) instruments have revolutionized the preparation of site-specific specimens for (scanning) transmission electron microscopy ((S)TEM) over the last 20 years. Initially, the first generation of single gallium beam instruments allowed easy site-specific preparation with sub-micron precision for the first time ever, although surface damage was a problem, and post treatment of the samples with things like low energy ion beams was required for highest surface quality. The second generation was dual electron and gallium ion beam instruments and these allowed reduction in surface damage due to being able to image the sample and deposit protective layers of amorphous Pt-C or other materials without causing ion beam damage. Progressive improvement of such instruments has included a reduction in the gallium beam energy allowing better final polishing, and improved nanomanipulators for easier *in-situ* liftout (a number of newer versions have been introduced by manufacturers in recent years allowing more flexible movement, rotation of the needle, and more user-friendly control). A third generation of FIB instruments suitable for (S)TEM specimen preparation is now being introduced in microscopy laboratories, based on a dual beam combination of a Xenon column and an electron column in a similar configuration to the dual beam gallium/electron column instruments. Whilst one major use of such instruments to date has been serial section tomography (Burnett, et al., 2016; Daly, et al., 2017; Kelly, et al., 2016), some recent studies have demonstrated the use of such Xe plasma FIB instruments for TEM specimen preparation (Garnier, et al., 2015; Giannuzzi & Smith, 2011; Hu, et al., 2017). This promises to bring several major advantages to TEM specimen preparation, since the use of Gallium ions comes with some notable downsides, including diffusing into group IV

---

† Now at Station Q Delft, Microsoft Corporation, Lorentzweg 1, 2628 CJ Delft, Netherlands

semiconductors (Ishitani, et al., 1998), interdiffusion and formation of non-stoichiometric regions in III-V semiconductors (Rubanov & Munroe, 2005; Wu, et al., 2009), and diffusion along grain boundaries in Al (Unocic, et al., 2010). It may also be the case that other more subtle chemical effects are contributing to surface amorphisation when performing FIB preparation with Ga beams. Whilst some previous studies have used final low-energy argon ion thinning of specimens lifted out with Ga FIB (for example, the doped bismuth ferrite used in two studies by the first author of this manuscript (MacLaren, et al., 2015; Yang, et al., 2017)), this only solves problems where the gallium damage is at the surface of the sample. Thus, it is going to be important to develop techniques for performing liftout on a wide range of materials using Xe PFIB, and to analyse the results carefully using (Scanning) Transmission Electron Microscopy. In this respect, the recent work of (Hu, et al., 2017) liftout of hydroxyapatite on Ti-6-4 with both Ga and Xe FIB is an important early contribution, and shows some relative advantages of the two technologies. It should also be noted that ex-situ liftout of Xe FIB specimens has been reported by (Giannuzzi, et al., 2015), although little TEM/STEM assessment of the results was carried out. In this work, we report on the use of a Xenon Plasma FIB with an *in-situ* nanomanipulator to lift out a thin section from a thin film of  $\text{La}_2\text{CoMnO}_6$  on (111)  $\text{SrTiO}_3$ , followed by the investigation of the quality of the resulting specimen using TEM and STEM.

## Experimental

A  $\text{La}_2\text{CoMnO}_6$  (LCMO) film was grown on a  $\text{SrTiO}_3$  (111) substrate by pulsed laser deposition using methods detailed elsewhere (Kleibeuker, et al., 2017). FIB preparation was performed using a Thermo Fisher Helios PFIB for Materials Science using a standard liftout method. Firstly, Pt was deposited to protect the area of interest using the electron beam deposition followed by Xenon beam deposition. Trenches were cut to either side using a 30 kV Xe beam with 1.3  $\mu\text{A}$  current for 2 min on each side. A 180 nA clean was then applied to each side for 1 min, followed by a 59 nA clean to each side for a further minute. This resulted in a specimen about 40  $\mu\text{m}$  wide, 25  $\mu\text{m}$  deep and 3-5  $\mu\text{m}$  wide. A “J-cut” was then made and the sample in this state is shown in Figure 1a. The sample was then bonded to a nanomanipulator needle with platinum, and then cut away and lifted out. It was then attached to a suitable copper support grid with Pt deposition (Figure 1b). Polishing of a section of this liftout about 3  $\mu\text{m}$  wide was performed at 30 kV at currents of 6.7 nA, 1.8 nA and 230 pA to thin the sample almost to the desired thickness. Final polishing was performed at 5 kV/200 pA and 2 kV / 200 pA until the edge was clearly receding and most likely electron transparent (Figure 1c). (Note, polishing of sections like this is common practice, since the thicker part of the liftout provides mechanical support to the thin part, and subsequent polishing of other parts of the section is possible later, if desired).

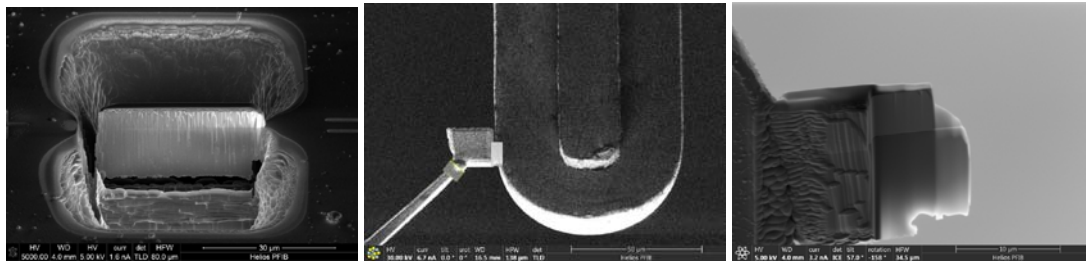


*Figure 1: FIB preparation in the Xenon plasma FIB: a) Sample after trenches have been cut, the sample has been polished to 3-5  $\mu\text{m}$  thickness and the J-cut has been made; b) bonding the sample to a grid; c) final thinned specimen.*

Initial Energy Filtered TEM results were obtained using a TITAN TEM/STEM operated at 300 KV. A probe  $C_s$  corrected TITAN operated at 300 kV with 22 mrad semi-convergence angle was used for STEM imaging. In order to avoid the beam damage, beam current was set to 25 pA, which is calibrated by built-in Faraday cage. ADF-STEM (25-100 mrad) and the newer iDPC-STEM imaging methods were employed simultaneously using a Fischione HAADF and a FEI 4-quadrant detector, respectively (Lazić, et al., 2016; Yücelen, et al., 2018).

Analysis of the peak positions in the atomic resolution images was performed using the Atomap software (Nord, et al., 2017).

## Results and Discussion

The sample showed a good-quality thin area, as shown in Figure 2a, which is an EFTEM map of relative thickness, showing a large area with thickness  $< 100$  nm (assuming the inelastic mean free path ( $\lambda$ ) is near to 100 nm) and a thin edge just a few nm thick. This sample appears at least as good as a high quality sample made using conventional Ga FIB liftout and low energy final thinning (see for example the sample used in Figure 6a of (Kleibecker, et al., 2017) which was finished with 5 kV Ga ions). More detail of the thin edge of the sample is shown in Figure 2b, showing that the sample is crystalline almost to the outer edge, with about 3 nm of amorphised material at the edge, which is comparable to the best results on oxide samples prepared using Ar ion milling or Ga FIB with 5 kV accelerating voltage (Kleibecker, et al., 2017; MacLaren & Richter, 2009).

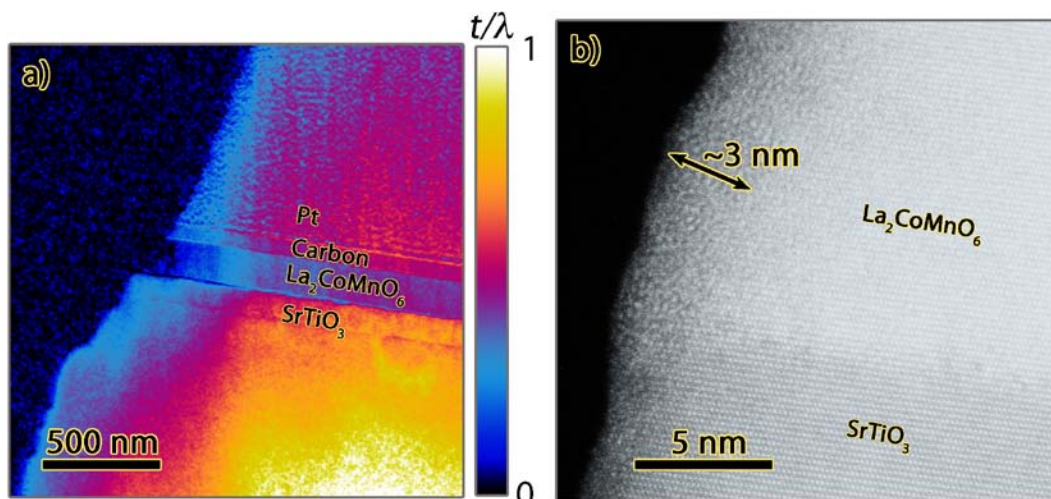


*Figure 2: TEM and STEM imaging of the sample edge: a) EFTEM  $t/\lambda$  map; b) HAADF STEM image showing a thin edge with about 3 nm of amorphised material.*

Figure 3 shows high-resolution STEM images recorded across the interface using standard HAADF imaging and the iDPC method with the sample oriented along a  $\langle 110 \rangle_{\text{cubic}}$  direction. Both images show an excellent quality sample with minimal surface roughness (which would show up as a modulation in the mean intensity of each distinct column type). Additionally, the iDPC-STEM image clearly reveals the oxygen atoms as well as the A-site Sr and La atoms and the B-site Ti, Mn, and Co atoms. It is clearly observed that the octahedra begin to tilt inside the LCMO layer, this tilting building up over several layers to a value somewhat like that expected for a well-ordered bulk LCMO material. This was observed and quantified for this thin film previously using Gaussian peak fitting of oxygen positions in annular bright field images (Kleibecker, et al., 2017).

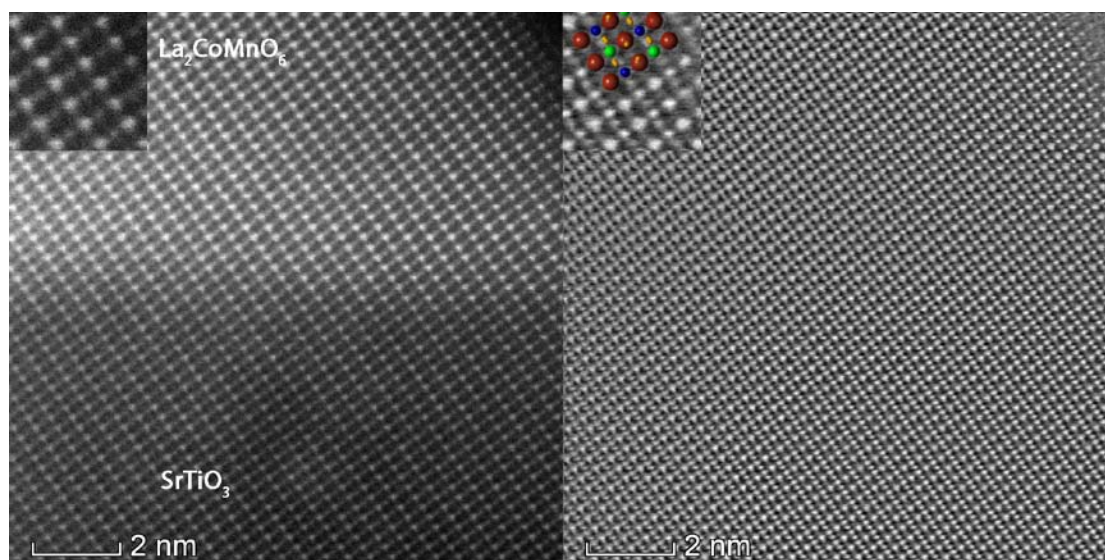


*Figure 3: a) HAADF and b) iDPC STEM images of the same area close to the sample edge showing excellent clarity of imaging of all atomic columns including A-site columns (La and Sr), B-site columns (Co/Mn and Ti) and O columns. More detail is shown in the insets, and the atoms are highlighted in the overlaid model where La - maroon, Co - blue, Mn - green, and O - orange.*

The quality of the iDPC-STEM imaging is so good that the atom positions were easy to quantify using the Atomap software (Nord, et al., 2017), which determines atom positions by 2D Gaussian profile fitting. The results of the analysis are then shown in Figure 4. In particular, the modulation of oxygen spacings resulting from the octahedral tilts is shown in this figure and shows the expected behavior (Kleibecker, et al., 2017). This conclusively demonstrates that this sample was of sufficient quality for quantitative atomic position quantification.



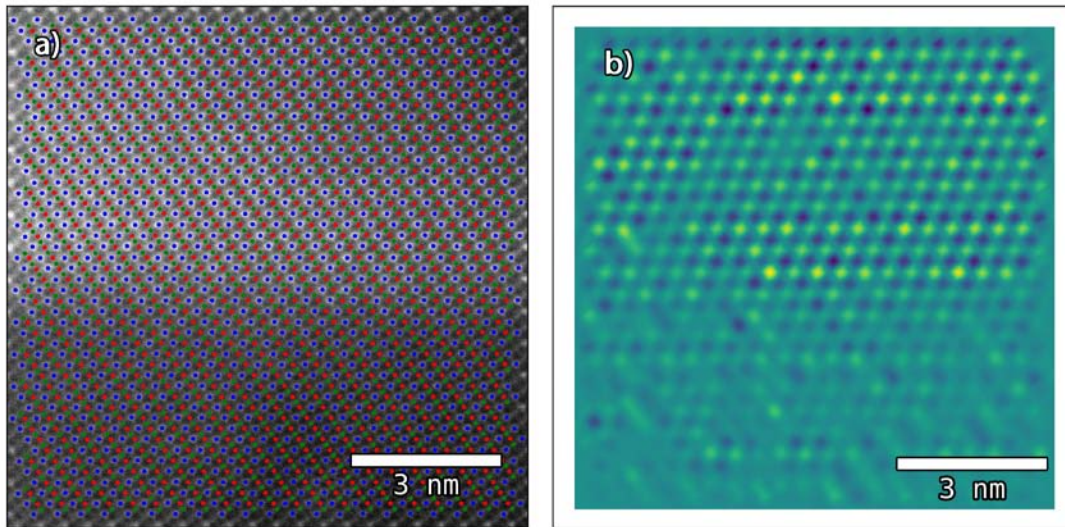


*Figure 4: Atomap analysis of atom positions from the images of Figure 3: a) atom positions found by the software; b) octahedral tilting as a function of position calculated from the oxygen atom positions.*

It is particularly interesting to note that the sample was prepared in just 3 hours, which is similar to the total time typically taken to prepare a liftout of the same material on an equivalent Ga FIB instrument. This was made possible by the very fast rough milling of the FIB trenches using the high currents available in the Xe PFIB (this is about 10 times faster than in a Gallium FIB of the same generation), even if the final thinning is slower (as the current density for low current beams is about 25 times lower than in an equivalent Ga FIB). It should also be noted that no external post-FIB preparation was necessary after the 2kV polish in the FIB. It is therefore clear that the Xe PFIB will be a powerful tool for the preparation of ultrahigh quality TEM lamellae suitable for atomic resolution imaging from a range of materials, including easily damaged materials like SrTiO<sub>3</sub> and other perovskites, and should not simply be seen as a tool for three dimensional reconstruction nor just for larger scale semiconductor processing. Further work will be required to determine how much advantage use of Xe-beam FIB gives to TEM/STEM specimen preparation of different classes of materials.

## **Conclusions**

A thin film of La<sub>2</sub>CoMnO<sub>6</sub> on a (111) SrTiO<sub>3</sub> substrate was prepared for TEM/STEM characterization using a focused ion beam liftout method using a Xenon ion beam in a dual beam instrument. In comparison with a similar preparation in a conventional Ga-beam FIB, the rough cut and liftout was faster, but the final thinning was slower, due to the broader beam at low currents with Xe. The resulting sample was found to be literally just a few nm thick at the outside edge, with just about 3 nm of amorphised material at the outside edge. Atomic resolution STEM imaging of this thin region using HAADF and iDPC imaging shows excellent quality imaging with very even contrast reflecting a very flat surface, and allowing simple automated evaluation of oxygen atom positions and visualization of octahedral tilting using a recently developed software package. This emphasizes that, even without any further post-finishing,

Xenon beam FIB shows excellent promise for sample preparation for the highest spatial resolution STEM and TEM characterization of materials.

### Acknowledgements

The authors are indebted to the EPSRC for the funding of this work via the project "A Focused Ion Beam Microscopy Facility for Advanced Materials Analysis" (Grant reference EP/P001483/1). Atomap was developed by Magnus Nord whilst employed as part of the project "Fast Pixel Detectors: a paradigm shift in STEM imaging" (Grant reference EP/M009963/1).

### References

- BURNETT, T.L., KELLEY, R., WINIARSKI, B., CONTRERAS, L., DALY, M., GHOLINIA, A., BURKE, M.G. & WITHERS, P.J. (2016). Large volume serial section tomography by Xe Plasma FIB dual beam microscopy. *Ultramicroscopy* **161**, 119-129.
- DALY, M., BURNETT, T.L., PICKERING, E.J., TUCK, O.C.G., LEONARD, F., KELLEY, R., WITHERS, P.J. & SHERRY, A.H. (2017). A multi-scale correlative investigation of ductile fracture. *Acta Mater.* **130**, 56-68.
- GARNIER, A., FILONI, G., HRNCIR, T. & HLADIK, L. (2015). Plasma FIB: Enlarge your field of view and your field of applications. *Microelectron. Reliab.* **55**(9-10), 2135-2141.
- GIANNUZZI, L.A. & SMITH, N.S. (2011). TEM Specimen Preparation with Plasma FIB Xe+ Ions. *Microsc. Microanal.* **17** [S2], 646-647.
- GIANNUZZI, L.A., YU, Z.Y., YIN, D., HARMER, M.P., XU, Q., SMITH, N.S., CHAN, L.S., HILLER, J., HESS, D. & CLARK, T. (2015). Theory and New Applications of Ex Situ Lift Out. *Microsc. Microanal.* **21**(4), 1034-1048.
- HU, C.M., AINDOW, M. & WEI, M. (2017). Focused ion beam sectioning studies of biomimetic hydroxyapatite coatings on Ti-6Al-4V substrates. *Surf. Coat. Technol.* **313**, 255-262.
- ISHITANI, T., KOIKE, H., YAGUCHI, T. & KAMINO, T. (1998). Implanted gallium ion concentrations of focused-ion-beam prepared cross sections. *J. Vac. Sci. Technol. B* **16**(4), 1907-1913.
- KELLY, M.N., GLOWINSKI, K., NUHFER, N.T. & ROHRER, G.S. (2016). The five parameter grain boundary character distribution of alpha-Ti determined from three-dimensional orientation data. *Acta Mater.* **111**, 22-30.
- KLEIBEUKER, J.E., CHOI, E.-M., JONES, E.D., YU, T.-M., SALA, B., MACLAREN, B.A., KEPAPTSOGLU, D., HERNANDEZ-MALDONADO, D., RAMASSE, Q.M., JONES, L., BARTHEL, J., MACLAREN, I. & MACMANUS-DRISCOLL, J.L. (2017). Route to achieving perfect B-site ordering in double perovskite thin films. *NPG Asia Materials* **9**, e406.
- LAZIĆ, I., BOSCH, E.G.T. & LAZAR, S. (2016). Phase contrast STEM for thin samples: Integrated differential phase contrast. *Ultramicroscopy* **160**, 265-280.
- MACLAREN, I. & RICHTER, G. (2009). Structure and possible origins of stacking faults in gamma-yttrium disilicate. *Philos. Mag.* **89**(2), 169-181.
- MACLAREN, I., WANG, L., MCGROUTHER, D., CRAVEN, A.J., MCVITIE, S., SCHIERHOLZ, R., KOVÁCS, A., BARTHEL, J. & DUNIN-BORKOWSKI, R.E. (2015). On the origin of differential phase contrast at a locally charged and globally charge-compensated domain boundary in a polar-ordered material. *Ultramicroscopy* **154**(0), 57-63.

- NORD, M., VULLUM, P.E., MACLAREN, I., TYBELL, T. & HOLMESTAD, R. (2017). Atomap: a new software tool for the automated analysis of atomic resolution images using two-dimensional Gaussian fitting. *Advanced Structural and Chemical Imaging* **3**, 9.
- RUBANOV, S. & MUNROE, P.R. (2005). Damage in III-V compounds during focused ion beam milling. *Microsc. Microanal.* **11**(5), 446-455.
- UNOCIC, K.A., MILLS, M.J. & DAEHN, G.S. (2010). Effect of gallium focused ion beam milling on preparation of aluminium thin foils. *J Microsc-Oxford* **240**(3), 227-238.
- WU, J.H., YE, W., CARDOZO, B.L., SALTZMAN, D., SUN, K., SUN, H., MANSFIELD, J.F. & GOLDMAN, R.S. (2009). Formation and coarsening of Ga droplets on focused-ion-beam irradiated GaAs surfaces. *Appl. Phys. Lett.* **95**(15), 3.
- YANG, H., MACLAREN, I., JONES, L., MARTINEZ, G.T., SIMSON, M., HUTH, M., RYLL, H., SOLTAU, H., SAGAWA, R., KONDO, Y., OPHUS, C., ERCIUS, P., JIN, L., KOVACS, A. & NELLIST, P.D. (2017). Electron ptychographic phase imaging of light elements in crystalline materials using Wigner distribution deconvolution. *Ultramicroscopy* **180**, 173-179.
- YÜCELEN, E., LAZIĆ, I. & BOSCH, E.G.T. (2018). Phase contrast scanning transmission electron microscopy imaging of light and heavy atoms at the limit of contrast and resolution. *Sci. Rep.-UK* **8**, 2676.